

## Finite-Size Effects in Single Chain Magnets: An Experimental and Theoretical Study

L. Bogani,<sup>1</sup> A. Caneschi,<sup>1</sup> M. Fedi,<sup>2</sup> D. Gatteschi,<sup>1</sup> M. Massi,<sup>2</sup> M. A. Novak,<sup>3</sup> M. G. Pini,<sup>4</sup>  
A. Rettori,<sup>5</sup> R. Sessoli,<sup>1,\*</sup> and A. Vindigni<sup>5</sup>

<sup>1</sup>*Dipartimento di Chimica and INSTM, Università di Firenze, I-50019 Sesto Fiorentino, Italy*

<sup>2</sup>*Dipartimento di Fisica and INFN, Università di Firenze, I-50019 Sesto Fiorentino, Italy*

<sup>3</sup>*Instituto de Física Universidade Federal do Rio de Janeiro, CP68528, RJ 21945-970, Brazil*

<sup>4</sup>*Istituto di Fisica Applicata "Nello Carrara," CNR, I-50019 Sesto Fiorentino, Italy*

<sup>5</sup>*Dipartimento di Fisica and INFN, Università di Firenze, I-50019 Sesto Fiorentino, Italy*

(Received 4 August 2003; published 21 May 2004)

The problem of finite-size effects in  $s = 1/2$  Ising systems showing slow dynamics of the magnetization is investigated introducing diamagnetic impurities in a  $\text{Co}^{2+}$ -radical chain. The static magnetic properties have been measured and analyzed considering the peculiarities induced by the ferrimagnetic character of the compound. The dynamic susceptibility shows that an Arrhenius law is observed with the same energy barrier for the pure and the doped compounds while the prefactor decreases, as theoretically predicted. Multiple spin reversal has also been investigated.

DOI: 10.1103/PhysRevLett.92.207204

PACS numbers: 75.40.Gb, 75.10.Hk, 76.90.+d

One of the open problems in low dimensional magnetism is the influence of finite-size effects [1,2]. The investigation of their role on dynamic properties, which are of great relevance for nanostructures, is particularly interesting. For the Ising spin chain Glauber proposed a stochastic dynamics [3] widely applied to a variety of phenomena. The experimental investigation of this dynamics in magnetic 1D compounds was prevented by the strict requirements the system must fulfill. Recently, molecular 1D materials were found to show magnetic hysteresis in the absence of long range magnetic order [4–6]. They have, thus, been named “single chain magnets” (SCMs) by analogy to slow relaxing 0D systems widely known as “single molecule magnets” (SMMs) [7]. The first of these compounds was  $\text{Co}(\text{hfac})_2\text{NitPhOMe}$  (CoPhOMe in the following) [4], made of alternating and interacting  $\text{Co}^{2+}$  ions (anisotropic effective  $s = 1/2$  spins) and nitronyl-nitroxide radicals (isotropic  $s = 1/2$  spins). The relaxation time follows an Arrhenius law as predicted by Glauber [3] for a 1D Ising system, with  $\tau = \tau_0 e^{\Delta/k_B T}$  and  $\Delta/k_B = 152$  K, for ten decades of time in the temperature range  $T = 4\text{--}15$  K [8].

The observation of Glauber dynamics in the paramagnetic phase of a real system represents a paradox. In fact, a strong Ising-type intrachain interaction is required because  $\Delta$  is proportional to the coupling constant  $J$ . On the other hand, the correlation length of the Ising model diverges exponentially at low temperature,  $\xi \sim \exp[(2J)/(k_B T)]$ , and favors the 3D ordering by enhancing the weak interchain interactions [9]. A possible explanation could be the presence of naturally occurring defects, which can geometrically limit the correlation length and dramatically reduce the 3D ordering temperature [9,10]. The presence of defects is known to affect also the dynamics of the magnetization, but direct investigations of their influence on the slow relaxing magnetization are still lacking. The persistence of slow dynamics even for

small segments of chains is an important result, making SCMs much more appealing than SMMs in many respects. Finite-size effects are commonly investigated through the insertion of breaks by doping with diamagnetic ions, but important aspects, such as the reproducibility or homogeneity of the concentration of the dopant, are often overlooked. We present here a thorough experimental and theoretical investigation of finite-size effects in the slow relaxing Ising chain CoPhOMe, thus evidencing the key role played by the defective sites in the nucleation of the excitation, similar to what is observed in quasi-1D oxides [1]. A shortcut of the Glauber barrier through coherent reversal of multiple spins is observable in the ac susceptibility thanks to the introduction of defects.

Variable concentrations of diamagnetic impurities have been inserted in the chains and the samples have been investigated with unprecedented accuracy. Doped crystals were prepared [11] adding to the solutions different ratios of  $\text{Zn}(\text{hfac})_2 \cdot 2\text{H}_2\text{O}$  vs  $\text{Co}(\text{hfac})_2 \cdot 2\text{H}_2\text{O}$  in the range 0–0.30. As a strongly inhomogeneous distribution of the dopant inside single crystals could be of major relevance for the magnetic properties, we used the particle induced x-ray emission technique (PIXE) with an external microbeam [12] to analyze the Zn doping profile. The low minimum detection limits of PIXE allowed us to find that no metals other than Co and Zn were present in concentrations  $> 12$  ppm, and thus no appreciable contribution could rise from paramagnetic impurities. The mean Zn/Co ratios of the investigated samples,  $c$ , were 0.003, 0.019, and 0.047, giving an average length  $\bar{L}$  between two  $\text{Zn}^{2+}$  ions variable from ca. 300 to ca. 20 spins. The Zn concentration was always found to be lower than the ratio of the starting solution and reproducible in crystals from the same batch (within an error of 5% on  $c$ ) but not reproducible in different syntheses. Using the microbeam, we could then monitor the spatial distribution of the

dopant inside individual crystals, a procedure never performed in studies of this kind. The results are shown in Fig. 1 for longitudinal and transversal scans. The former shows uniformly distributed impurities, while the latter shows that the Zn concentration slightly increases going from the center to the edges. This observation is consistent with a progressive enriching of the solution in Zn content.

The magnetic susceptibility of a chain in a moderate field is strongly sensitive to geometrical limitations of the correlation length. In Fig. 2 (top), we report the temperature dependence of the real component  $\chi'$  of the ac magnetic susceptibility measured at 2.7 kHz in a static magnetic field  $H = 2$  kOe along the easy axis for an undoped crystal and for two doped samples. In contrast with magnetic data and theoretical calculations reported thus far for chains, which show the presence of only one peak [13–15], evident is the presence of a large anomalous structure with two peaks for  $T \approx 33$  K and for  $T \approx 14$  K (below the blocking temperature  $T_b \approx 12$  K, we observe frequency dependent dynamical effects). The higher temperature peak roughly corresponds to that expected for an infinite 1D Ising system in the presence of a field [see Fig. 2 (bottom)] and shifts to higher temperature on increasing the field, as expected. This peak is more pronounced in the pure sample and decreases and shifts to lower temperatures with higher dopings, while the lower temperature peak increases. At high doping (0.047) only this latter peak survives. This unprecedented behavior can be explained solving the randomly diluted ferrimagnetic Ising chain in field. The spin Hamiltonian we have used is

$$\mathcal{H} = - \sum_{i=1}^{L/2} \left( J(\sigma_{2i-1}\sigma_{2i} + \sigma_{2i}\sigma_{2i+1}) + \frac{\mu_B H}{2} (g_{Co}\sigma_{2i} + g_R\sigma_{2i-1}) \right), \quad (1)$$

where  $g_{Co}$  and  $g_R$  are the Landé factors of Co and radical spins,  $\mu_B$  is the Bohr magneton,  $H$  is the external mag-

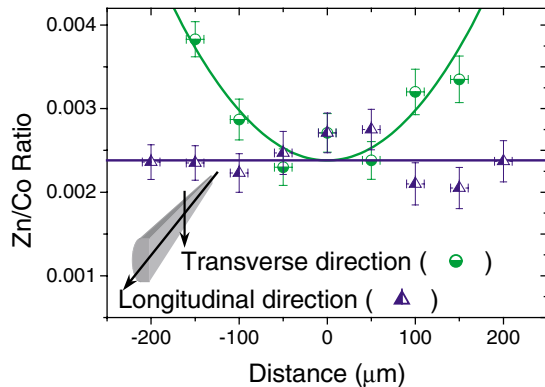


FIG. 1 (color online). Zn/Co ratio in a single crystal of CoPhOMe. The distribution of the dopant is reported for both longitudinal and transversal directions, scanned as shown in the drawing. Lines are guides to the eye.

netic field, and  $\sigma_i = \pm 1$ , except for  $\sigma_{L+1} = 0$ . Within a transfer matrix formalism, which is reported in the literature [13–15], the free energy of a segment of length  $L$  can be obtained. The thermodynamic observables are calculated summing all the  $L$ 's weighted by the probability of occurrence of that length:  $P_L = c^2(1-c)^L$  [13].

In Fig. 2 (bottom), we report the calculated magnetic susceptibility  $\chi(T)$  for  $J/k_B = -90$  K,  $H = 2$  kOe,  $g_{Co} = 7$ , and  $g_R = 2$  and for different doping values. For the infinite chain we obtain only one peak at  $T \approx 34$  K, which shows the observed trend with field, while the introduction of nonmagnetic impurities gives rise to the observed peak shift and to a shoulder at about 15 K. This feature, which eventually develops into a single peak at high doping, is mainly due to the finite-size contribution to the free energy [13], as will be shown in a forthcoming work. Although complete quantitative agreement is not possible due to the helicoidal structure of the CoPhOMe chain [8,11], the overall behavior and the anomalous feature are well reproduced by the simple model expressed by (1). This is especially true if one introduces, at low concentrations, a parabolic distribution

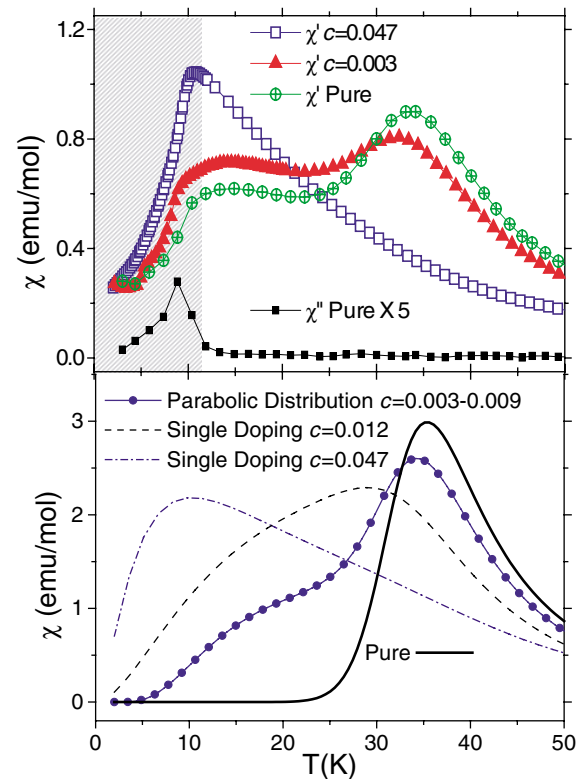


FIG. 2 (color online). Top: Temperature dependence of the longitudinal magnetic ac susceptibility (2.7 kHz) measured for different dopings in a static field of 2 kOe with an ac field of 10 Oe. Data for other frequencies in the 10 Hz–10 kHz range are not reported because  $\chi'$  is frequency dependent only in the shaded area. Bottom: Calculated susceptibility (parameters in the text) for different concentrations of impurities. A parabolic distribution is used, at low concentrations, to account for the observed transversal trend.

of the dopant, as in Fig. 1, while at higher concentrations the behavior can be reproduced using either a distribution or homogeneous doping.

The presence of the low temperature peak even in the pure compound suggests that other types of defects are indeed present beyond the introduced Zn impurities. Both crystalline defects and chemical modifications (due to a certain lability of the organic radicals) are present in the undoped compound and are expected to be more concentrated close to the crystal surface, as for the dopant. These data suggest a concentration of defects in the pure compound of the order of a few per thousand, a value that agrees well with the calculated curves of Fig. 2 and the following discussion on the dynamics.

The dynamics of the magnetization of the pure and doped samples has been investigated measuring the temperature dependence of the real ( $\chi'$ ) and imaginary ( $\chi''$ ) components of the ac susceptibility for seven different frequencies in the range 10 Hz–10 kHz.  $\chi''$  displays a maximum whose position depends on the frequency  $\omega$  of the applied ac field, and the relaxation time can thus be extracted [8]:  $\tau^{-1}(T_{\max}) = \omega$ . For the highest concentration the curves become more distorted, with a small shoulder at low temperature. The results are plotted in Fig. 3 in the  $\ln(\tau)$  vs  $1/T$  scale. A linear behavior is observed for all compounds and the slope (i.e., the barrier  $\Delta$  of the Arrhenius law) remains substantially unchanged ( $160 \pm 8$  K). The fitted lines shift down on increasing the doping with the preexponential factor  $\tau_0$  going from  $3.5 \times 10^{-11}$  s for the pure compound to  $1.0 \times 10^{-12}$  s when  $c = 0.047$ .

In order to reproduce theoretically the data of Fig. 3, we assumed the simplified model of a dilute ferromagnetic chain (in a ferrimagnet only an equivalent ferromagnetic branch with  $J = |J|$  and  $g = g_{Co} - g_R$  is effective for the slow relaxation [8]). For an open chain of length  $L$ , the time evolution of the expectation values of the spins can be described by the matrix equation:

$$\frac{\partial}{\partial t} \mathbf{S} = -\mathbf{M}\mathbf{S}, \quad (2)$$

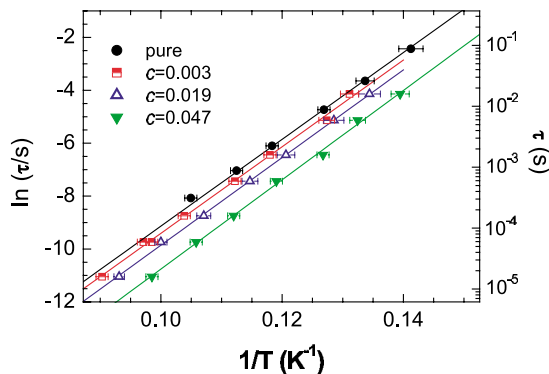


FIG. 3 (color online). Relaxation time of the magnetization extracted from the longitudinal ac susceptibility measured in zero static field for different concentrations of Zn.

where  $\mathbf{M}$  is a tridiagonal matrix. The time scale of the relaxation process  $\tau_L(T)$  is related to the smaller eigenvalue of  $\mathbf{M}$ . In the range of  $\xi$  and  $L \gg 1$  asymptotic expansions for this eigenvalue are given in literature, leading to  $\tau_L(T) \sim \xi^2$  if  $\xi \ll L$ , and  $\tau_L(T) \sim L\xi$  if  $\xi \gg L$  [16,17]. However, as the experimental  $\tau$  is extracted from the ac susceptibility of an ensemble of segments with different length, we need to evaluate  $\tau_L$  for any  $L$  and  $T$ . The eigenvalue spectrum of  $\mathbf{M}$  can be expressed as

$$\lambda_L(\theta) = q\alpha_0[1 - \gamma \cos(\theta)], \quad (3)$$

where  $q$  is the probability of reversal of the isolated spin per unit time  $\alpha_0^{-1}$ ,  $\gamma = \tanh[(2J)/(k_B T)]$ , and by  $\theta$  we denote the  $L$  possible roots of the trigonometric Eq. 2.6 of Ref. [17]. The relaxation time of the segment of length  $L$  is related to the smallest nonzero root  $\theta_0$  via  $\tau_L(T) = \lambda_L^{-1}(\theta_0)$ , while the root  $\theta = 0$  is rejected since it provides the relaxation time of the infinite chain. We introduced  $\tau_L(T)$  in the average susceptibility:

$$\chi(\omega, T) = \frac{\sum_{L=1}^{\infty} P_L \chi_L(T) [1 - i\omega\tau_L(T)]^{-1}}{\sum_{L=1}^{\infty} P_L}, \quad (4)$$

where  $\chi_L$  is the susceptibility of a ferromagnetic Ising segment of length  $L$  [14]. We extracted the relaxation time of the randomly doped sample from the maximum of the imaginary component of the computed ac susceptibility. In Fig. 4, we show the Arrhenius plots thus obtained for different concentrations of dopant. A crossover between the two regions with  $\bar{L} \gg \xi$  and  $\bar{L} \ll \xi$  is observed and the slope is halved in the latter case, where the concentration of impurities  $c$  affects only the offset of the curves. This is consistent with a relaxation process where a domain wall is nucleated at an end point of a segment  $L$ , with a halved energy cost  $2J$ , and has the probability  $\frac{1}{L}$  to reach the other end point [18], leading to the linear dependence of the relaxation time on the size of the system.

The experimental data of Fig. 3 scale with  $c$  as the calculated curves when  $\bar{L} \ll \xi$ , thus evidencing that

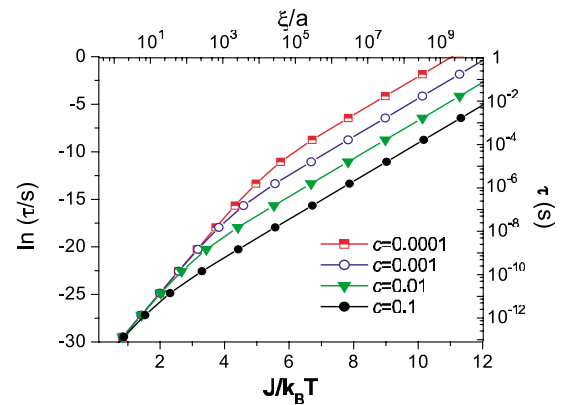


FIG. 4 (color online). Calculated temperature dependence of the relaxation time extracted from  $\chi(\omega, T)$  with  $\alpha_0 = 3.6 \times 10^{13} \text{ s}^{-1}$  and  $q = 0.73$ . To compare with data in Fig. 3, assume  $J/k_B = 80$  K.

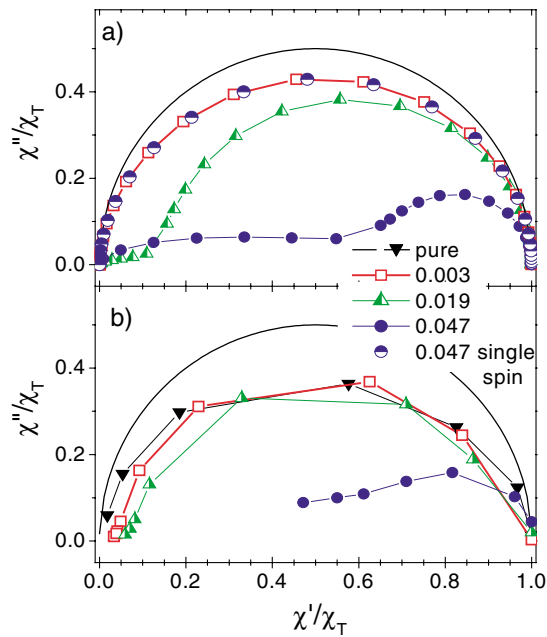


FIG. 5 (color online). (a) Calculated Cole-Cole plot for different concentrations of randomly distributed diamagnetic impurities at  $T = 8$  K assuming  $J/k_B = 80$  K,  $q = 0.73$ , and  $\alpha_0 = 3.6 \times 10^{13} \text{ s}^{-1}$ . The half-filled circles stay for  $c = 0.047$  without multiple spin reversal. (b) Experimental data at  $T = 8$  K for the four investigated samples.

finite-size effects are also present in the nominally pure compound. Although a direct analysis of its defects is not possible, by comparing the values of  $\tau_0$  we estimate an average length of the chains in the undoped sample of the order of a thousand spins (as deduced from the analysis of the susceptibility in a moderate field). The geometrical reduction of  $\xi$  can be responsible for the suppression of long range magnetic order in CoPhOMe [9,10]. The measured activation energy  $\Delta$  thus corresponds to  $2J$  instead of  $4J$ , leading to  $J/k_B = 80$  K, in good agreement with the simulation of the susceptibility data of Fig. 2.

Until now, we have neglected a relaxation mechanism which involves the simultaneous reversal of all the  $L$  spins of a segment, whose probability scales as  $q^L$  and therefore is relevant for short segments. This term can be added to  $\lambda_L(\theta_0)$  to obtain the probability to relax in the unit time  $\alpha_0^{-1}$ . Clear evidence of such a relaxation mechanism appears in the Cole-Cole plot [Fig. 5(a)], where  $\chi''$  vs  $\chi'$  is reported. In the absence of a distribution of relaxation times, the curve is expected to be a semicircle with the center on the  $x$  axis. A distribution in  $\tau$ , induced by the random doping, has the only effect to slightly push the center down, even for the highest doping. On the contrary, the coherent reversal of all the spins gives rise to a more complex behavior. The calculated curves of Fig. 5(a) are in fact well below the semicircle and show a flat region for higher frequencies where  $\chi' \rightarrow 0$ . This effect is particularly evident for high doping. The experimental results are shown in Fig. 5(b). Although the range

of available frequencies is limited, the agreement between observed and calculated curves suggests that coherent reversal of all the spins is experimentally observed for short segments. An accurate investigation on the temperature dependence of  $q$  could discriminate between a thermally activated and a tunneling process.

In conclusion, we have shown that finite-size effects are important in magnetic bistable 1D nanostructures halving the energy barrier predicted by the Glauber model. We observe a linear dependence of the relaxation time on the size of the system, which is completely different from the exponential dependence on the square of the spin value observed in SMMs, or the exponential dependence on the volume in single domain particles. This opens the possibility to employ segments of chains, even without a precise control on the length, as nanometric magnetic memory units characterized by a higher  $T_b$  and a larger magnetic moment than those obtained in SMMs. Moreover, a nonthermally activated relaxation could be observed for short segments. To better investigate this phenomenon, higher doping is required but it cannot be obtained with the present chemical approach. Synthesis in confined media as well as the organization of segments on surfaces, as already done for metallic Co nanowires on Pt surfaces [19], are under investigation.

Financial support from Italian MIUR (Fondi FISIR and FIRB), German DFG, and Brazilian CAPES, CNPq, and Instituto de Nanociencias is gratefully acknowledged.

\*Author to whom correspondence should be addressed.

Electronic address: roberta.sessoli@unifi.it

- [1] G. Xu *et al.*, Science **289**, 4192 (2000).
- [2] S. Eggert *et al.*, Phys. Rev. Lett. **89**, 047202 (2002).
- [3] R. J. Glauber, J. Math. Phys. (N.Y.) **4**, 294 (1963).
- [4] A. Caneschi *et al.*, Angew. Chem., Int. Ed. Eng. **40**, 1760 (2001).
- [5] R. Clerac *et al.*, J. Am. Chem. Soc. **124**, 12837 (2002).
- [6] R. Lescouëzec *et al.*, Angew. Chem., Int. Ed. Eng. **42**, 1483 (2003).
- [7] D. Gatteschi and R. Sessoli, Angew. Chem., Int. Ed. Eng. **42**, 268 (2003).
- [8] A. Caneschi *et al.*, Europhys. Lett. **58**, 771 (2002).
- [9] D. Hone *et al.*, Phys. Rev. B **12**, 5141 (1975).
- [10] C. Dupas *et al.*, Phys. Rev. B **25**, 3261 (1982).
- [11] A. Caneschi *et al.*, Dalton Trans. **21**, 3907 (2000).
- [12] M. Massi *et al.*, Nucl. Instrum. Methods Phys. Res., Sect. B **190**, 276 (2002).
- [13] M. Wortis, Phys. Rev. B **10**, 4665 (1974).
- [14] F. Matsubara *et al.*, Can. J. Phys. **51**, 1053 (1973).
- [15] M.G. Pini and A. Rettori, Phys. Lett. A **127**, 70 (1988).
- [16] J. Kamphorst Leal da Silva *et al.*, Phys. Rev. E **52**, 4527 (1995).
- [17] J.H. Luscombe *et al.*, Phys. Rev. E **53**, 5852 (1996).
- [18] R. Cordery *et al.*, Phys. Rev. B **24**, 5402 (1981).
- [19] P. Gambardella *et al.*, Nature (London) **416**, 301 (2002).